

# Dominant $T = 1$ channel proton-neutron interaction responsible for level structures of particle-hole nuclei around $^{100}\text{Sn}$

M. L. Liu, Y. H. Zhang, X. H. Zhou, J. J. He, X. G. Lei, Y. H. Qiang, L. He, and Z. G. Wang  
*Institute of Modern Physics, Chinese Academy of Sciences, Lanzhou 730000, People's Republic of China*  
 (Received 17 May 2011; revised manuscript received 6 September 2011; published 7 November 2011)

Near yrast positive-parity states of particle-hole nuclei around  $^{100}\text{Sn}$  have been studied and found mainly to be the coupling of  $g_{9/2}$  valence-proton holes to the  $d_{5/2}$  and  $g_{7/2}$  valence-neutron particles. The much higher excitation energy for a stretched coupled state involving  $\nu g_{7/2}$  rather than  $\nu d_{5/2}$  indicates that level structures of particle-hole nuclei around  $^{100}\text{Sn}$  might be dominated by the  $T = 1$  channel of proton-neutron residual interaction. The near yrast states are compared with the results of shell model calculations in the model space of  $\pi(p_{1/2}, g_{9/2})^{-1-4}$  and  $\nu(d_{5/2}, s_{1/2}, d_{3/2}, g_{7/2}, h_{11/2})^{1-3}$  by using the dominant  $T = 1$  channel proton-neutron quadrupole interaction; and the reasonable agreement with each other gives indirect proof of it being responsible for level structures of particle-hole nuclei around  $^{100}\text{Sn}$ .

DOI: [10.1103/PhysRevC.84.054306](https://doi.org/10.1103/PhysRevC.84.054306)

PACS number(s): 21.10.Re, 23.20.Lv, 27.70.+q

## I. INTRODUCTION

The study of level structures for nuclei near the proton drip line is a challenge for experimental nuclear physicists. Actually, much effort has been recently devoted to such meaningful investigations as nuclei near the shell closures at  $N = Z = 50$  [1–10]. Relevant spectroscopic data could improve knowledge of the realistic interaction in particle-hole nuclei around the doubly magic self-conjugate  $^{100}\text{Sn}$ . It is generally believed that the proton-neutron ( $p$ - $n$ ) interaction plays an important role in the evolution of nuclear structure. The quadrupole interaction is a main component of the  $p$ - $n$  residual interaction after extracting the monopole term, which includes the isospin singlet  $T = 0$  and triplet  $T = 1$  channels. Although the  $p$ - $n$  interaction for nuclei around  $^{100}\text{Sn}$  has been studied [11], a survey of the influence of the  $p$ - $n$  interaction, especially the isospin  $T = 0$  and  $T = 1$  channels, on high-spin level structures of particle-hole nuclei around  $^{100}\text{Sn}$  is still missing. Particle-hole nuclei around  $^{100}\text{Sn}$  have a few valence proton holes and neutron particles outside the proton ( $Z = 50$ ) and neutron ( $N = 50$ ) shell closures. They are expected to be spherical and can be interpreted in terms of multinucleon shell model configurations. In this work, we will examine which channel is dominated in the  $p$ - $n$  residual interaction and subsequently forms level structures of particle-hole nuclei around  $^{100}\text{Sn}$  [1–10] by comparing the experimental near yrast states to the corresponding shell model calculated ones in the model space of  $\pi(p_{1/2}, g_{9/2})^{-1-4}$  and  $\nu(d_{5/2}, s_{1/2}, d_{3/2}, g_{7/2}, h_{11/2})^{1-3}$ .

## II. DOMINANT $T = 1$ CHANNEL $p$ - $n$ INTERACTION

The Fermi levels for particle-hole nuclei around  $^{100}\text{Sn}$  lie at the  $\pi g_{9/2}^{-1}$  and  $\nu d_{5/2}$  orbitals. The  $\nu g_{7/2}$  comes very close to the Fermi surface. A study of low-lying energy levels in odd-odd nuclei in this region could provide useful information on the nature of the residual interaction between  $\pi g_{9/2}^{-1}$  and  $\nu d_{5/2}$  as well as  $\nu g_{7/2}$ . Figure 1 exhibits the experimental  $\pi g_{9/2}^{-1}\nu d_{5/2}$  and  $\pi g_{9/2}^{-1}\nu g_{7/2}$  multiplets for odd-odd nuclei

around  $^{100}\text{Sn}$ , where the  $J_{\max} - 1$  or  $J_{\max} - 2$  member is favored in energy to form the ground state. The data are taken from the Evaluated Nuclear Structure Data File [12]. As regards the two  $2^+$  states in  $^{98}\text{Ag}$ , we refer to Refs. [11, 12]. In addition, we tentatively use the 1290.6-keV level as  $1^+$  state in  $^{98}\text{Ag}$  [12].

The particle-hole interaction energy should be positive on average and strongest with extreme spin coupling. Starting from a general central interaction which acts on the spatial symmetric (antisymmetric)  $p$ - $n$  wave function, one would expect that enhanced (counteracted) interaction energy arising from the interplay of the configuration and its exchange counterpart. This is really true for the  $\delta$  interaction, which only allows the spatial-symmetric wave function to give a nonzero value. A state equally mixed by the spatial-symmetric and spatial-antisymmetric components would therefore become spatial-symmetric predominant after the action by the general central interaction. The proton  $g_{9/2}$  hole is strongly repulsive with the neutron  $d_{5/2}$  ( $g_{7/2}$ ) particle for the fully aligned  $7^+$  ( $8^+$ ) state, where the  $7^+$  state is the pure spin triplet  $S = 1$  according to the  $L$ - $S$  coupling and the  $8^+$  state is the mixing of the spin triplet  $S = 1$  and singlet  $S = 0$ . If the  $7^+$  and  $8^+$  states are spatial-symmetric prominent, the former should be governed by the  $T = 0$  ( $S = 1$ ) component based on the overall antisymmetry under the exchange of proton and neutron indices. The much higher excitation energy for fully aligned  $8^+$  state rather than  $7^+$  state (see Fig. 1) implies that the  $p$ - $n$  interaction for nuclei around  $^{100}\text{Sn}$  should not be dominated by the  $T = 0$  channel.

Figure 2 shows the pure  $T = 0$  and  $T = 1$  proton hole-neutron particle interactions for configurations  $\pi g_{9/2}^{-1}\nu d_{5/2}$  and  $\pi g_{9/2}^{-1}\nu g_{7/2}$  with quadrupole-quadrupole force  $\chi_2 = \frac{-400}{A^{5/3}}$  [13]. A parameter  $\alpha$  is employed in the  $p$ - $n$  interaction to set the strength partition between the isospin  $T = 0$  and  $T = 1$  channels:  $\chi_2^{T=0} = 2\alpha \frac{-400}{A^{5/3}}$  and  $\chi_2^{T=1} = 2(1 - \alpha) \frac{-400}{A^{5/3}}$ .  $\alpha = 1$  ( $\alpha = 0$ ) represents the pure  $T = 0$  ( $T = 1$ ) proton hole-neutron particle interaction. The  $T = 1$   $p$ - $n$  interactions are somewhat similar to those derived from CD-Bonn potential,

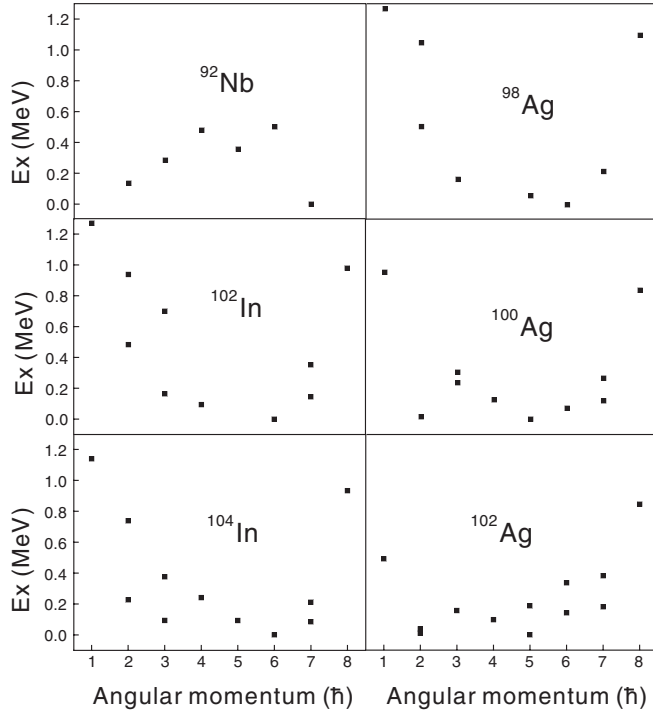


FIG. 1.  $\pi g_{9/2}^{-1} \nu d_{5/2}$  and  $\pi g_{9/2}^{-1} \nu g_{7/2}$  multiplets for odd-odd nuclei around  $^{100}\text{Sn}$  dominated by the  $T = 1$  channel of  $p$ - $n$  interaction. For the purpose of comparison, we also give the complete  $\pi g_{9/2} \nu d_{5/2}$  multiplet for  $^{92}\text{Nb}$  dominated by the  $T = 0$  channel of the  $p$ - $n$  interaction.

which are in good agreement with the experimental observed multiplet members [11]. It is shown in Fig. 2 that the maximum spin  $8^+$  state is well separated from two close  $7^+$  states mixed by  $\pi g_{9/2}^{-1} \nu d_{5/2}$  and  $\pi g_{9/2}^{-1} \nu g_{7/2}$  configurations when the  $p$ - $n$  interaction is dominated by the  $T = 1$  channel, i.e.,  $\alpha < 0.5$ . This is consistent with the experimental results in odd-odd nuclei in this region. As a comparison, however, the  $7^+$  state is much lower in energy than the other members of the  $\pi g_{9/2} \nu d_{5/2}$  multiplet in  $^{92}\text{Nb}$  (see Fig. 1). Thus, the  $p$ - $n$  interaction in  $^{92}\text{Nb}$  might be dominated by the  $T = 0$  channel.

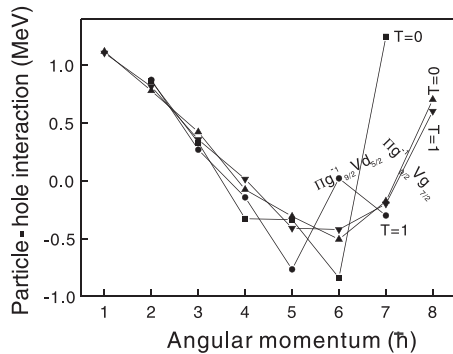


FIG. 2. Pure  $T = 0$  and  $T = 1$  interaction energy between  $g_{9/2}$  proton hole and ( $d_{5/2}$ ,  $g_{7/2}$ ) neutron particle vs angular momentum and, excitation energies of the  $7^+$  and  $8^+$  states as a function of the strength partition parameter  $\alpha$ , where 200 keV is used for the  $\nu g_{7/2}$  excitation energy.

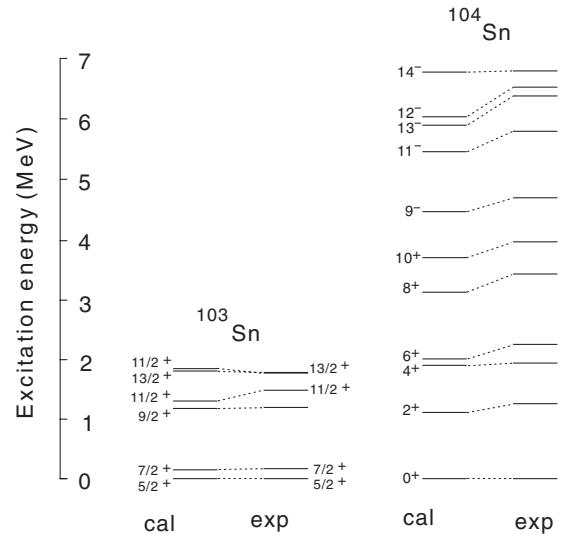
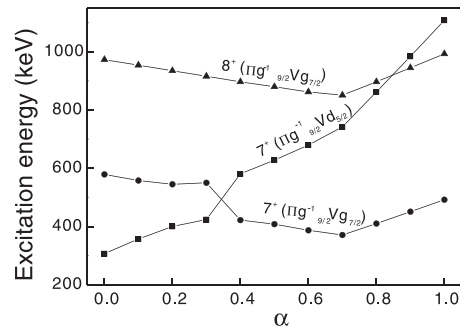


FIG. 3. Comparison of experimental and calculated energy levels of  $^{103,104}\text{Sn}$ .

### III. OUTLINE OF THE SHELL MODEL CALCULATIONS

Shell model calculations have been performed by using the code NUSHELLX [14]. The valence proton holes and neutron particles are confined in the  $\pi(p_{1/2}, g_{9/2})$  and  $\nu(d_{5/2}, s_{1/2}, d_{3/2}, g_{7/2}, h_{11/2})$  model space. By consulting the single-particle energies in Ref. [11], we fixed their energies in MeV as follows:  $\varepsilon_{\pi g_{9/2}^{-1}} = 0.0$ ,  $\varepsilon_{\pi p_{1/2}^{-1}} = 0.7$ ,  $\varepsilon_{\nu d_{5/2}} = 0.0$ ,  $\varepsilon_{\nu s_{1/2}} = 2.2$ ,  $\varepsilon_{\nu d_{3/2}} = 2.3$ ,  $\varepsilon_{\nu h_{11/2}} = 2.70$  except for  $\varepsilon_{\nu g_{7/2}} = 0.172$  MeV extracted from  $^{101}\text{Sn}$  [15].

The second step is then pursued for the proper like-nucleon interactions. The Gloeckner-Serduke interaction is suitable for the proton-proton channel [16]. The extended  $P + QQ$  interaction is adopted for the neutron-neutron channel [17,18]. We decide force strengths of the extended  $P + QQ$  interaction (in MeV):  $g_0 = 20/A$ ,  $g_2 = 225/A^{5/3}$ ,  $\chi_2 = 250/A^{5/3}$ ,  $\chi_3 = 350/A^6$  [13] for single-closed-shell Sn isotopes. As shown in Fig. 3, calculated level energies of  $^{103}\text{Sn}$  and  $^{104}\text{Sn}$  are in good agreement with the experimental ones [19,20]. Note that the calculated (experimental) excitation energies for  $2^+$ ,  $4^+$ , and



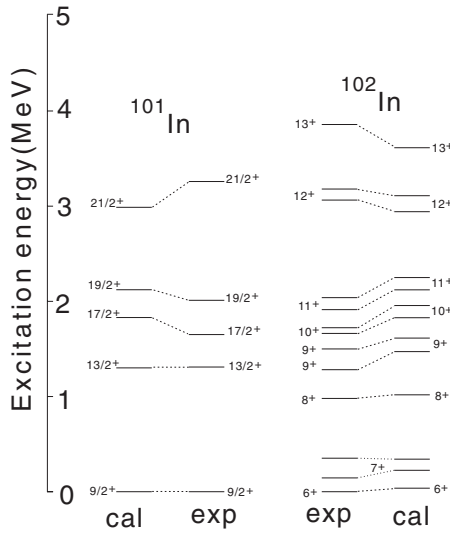


FIG. 4. Comparison of experimental and calculated positive-parity energy levels of  $^{101,102}\text{In}$ .

$6^+$  in  $^{102}\text{Sn}$  are located at 1313 (1472), 1983 (1969), and 1937 (2017) keV [21], respectively.

After that, we choose the dominating  $T = 1$  channel quadrupole-quadrupole force as the proton hole-neutron particle residual interaction. In a practical parameter search, the quadrupole-quadrupole force with strength  $\chi_2^{T=1} = 2(1 - \alpha)\frac{400}{A^{5/3}}$  ( $\alpha < 0.5$ ) [13] is set to optimally reproduce the observed energy levels of particle-hole nuclei around  $^{100}\text{Sn}$  as a whole. Here  $\alpha = 0.2, 0.275, 0.35,$  and  $0.425$  is linearly scaled for In, Cd, Ag, and Pd isotopes; in this case the  $p$ - $n$  interaction for  $^{92}\text{Nb}$  will be dominated by the  $T = 0$  channel (see Fig. 1). When  $\alpha$  is around  $0.2 \sim 0.425$ , the calculation can better reproduce the two close  $7^+$  states and well-separated  $7^+$ - $8^+$  spacing. The large overlap between the spin-orbit-partner orbitals  $\pi g_{9/2}^{-1}$  and  $\nu g_{7/2}$  leads to strong  $p$ - $n$  repulsion on average. In order to scale the increase of the  $\nu g_{7/2}$  single-particle excitation energy when the proton holes gradually fill the  $g_{9/2}$  orbital from  $Z = 50$  to  $Z = 40$  [22], we add two monopole corrections to the  $p$ - $n$  interaction  $\Delta k^{T=1}(\pi g_{9/2}^{-1}, \nu g_{7/2}) = \Delta k^{T=0}(\pi g_{9/2}^{-1}, \nu g_{7/2}) = 0.1$  in MeV. In Ref. [11], the realistic effective interaction derived from the

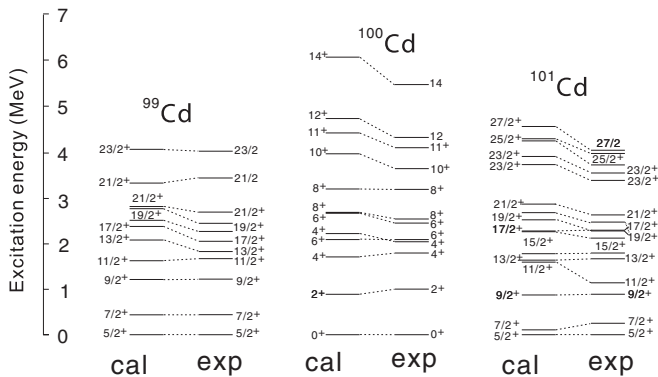


FIG. 5. Comparison of experimental and calculated positive-parity energy levels of  $^{99-101}\text{Cd}$ .

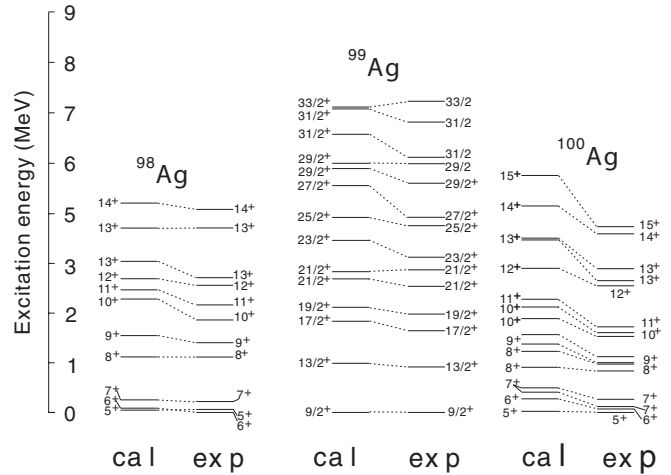


FIG. 6. Comparison of experimental and calculated positive-parity energy levels of  $^{98-100}\text{Ag}$ .

CD-Bonn  $NN$  potential for the fully aligned  $(\pi g_{9/2}^{-1} \nu g_{7/2})_{8^+}$  state lies at  $\sim 1.8$  MeV higher than that of the  $(\pi g_{9/2}^{-1} \nu g_{7/2})_{7^+}$  state. If a strong correction  $\Delta k^{T=1}(\pi g_{9/2}^{-1} \nu g_{7/2})_{8^+} = 1, 0.75, 0.5,$  and  $0.25$  MeV is set for In, Cd, Ag, and Pd isotopes, we can improve the positions of the fully aligned states involving  $\nu g_{7/2}$  greatly [in order to be consistent with  $\alpha$ , we tentatively use the linear scaling of  $\Delta k^{T=1}(\pi g_{9/2}^{-1} \nu g_{7/2})_{8^+}$  for simplicity]. The same set of parameters is employed for calculations for the isotopes.

The comparisons between the experimental and theoretical energy levels are shown in Figs. 4–8. Tables I, II, III, and IV show the leading component of configurations  $(p^{-1} \dots 4)_{J_p}^{\pi} (n^{-1} \dots 3)_{J_n}^{\pi}$  ( $\pi$  being the parity of proton and neutron subsystems), its squared amplitudes, and expectation values of proton numbers  $\langle n_a \rangle_p$  and neutron numbers  $\langle n_a \rangle_n$  in the respective orbitals  $a$ . It can be seen from Figs. 4–8 that the overall agreement is satisfactorily good for both the positive- and negative-parity states.

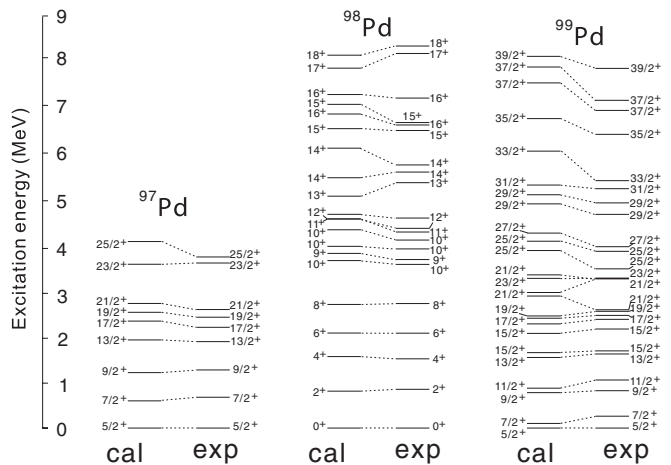


FIG. 7. Comparison of experimental and calculated positive-parity energy levels of  $^{97-99}\text{Pd}$ .

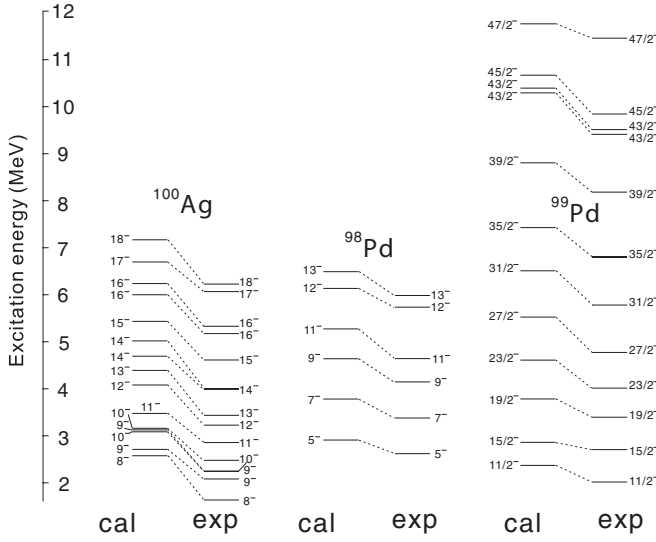


FIG. 8. Comparison of experimental and calculated negative-parity energy levels of  $^{100}\text{Ag}$  and  $^{98,99}\text{Pd}$ .

#### IV. LEVEL STRUCTURES OF PARTICLE-HOLE NUCLEI AROUND $^{100}\text{Sn}$

##### A. Level structure of positive-parity states in $^{101-102}\text{In}$

It is expected that the levels in  $^{101-102}\text{In}$  [1,2] may be associated with the  $\pi g_{9/2}^{-1} \nu(d_{5/2}g_{7/2})^{2-3}$  configuration in terms of the active high- $j$  orbitals around the Fermi levels mentioned above. The  $13/2^+$  state in  $^{101}\text{In}$  is mainly constructed by the

$\nu(d_{5/2}^2)_{2^+}$  coupled to the  $\pi g_{9/2}^{-1}$ . It can be seen from Table I that the  $17/2^+$  state in  $^{101}\text{In}$  is the coupling of the  $\nu(d_{5/2}g_{7/2})_{6^+}$  rather than  $\nu(d_{5/2}^2)_{4^+}$  excitation to the  $\pi g_{9/2}^{-1}$ . This is due to the defect that the extended  $P + QQ$  interaction gives an inverse order of the  $4^+$  and  $6^+$  levels in  $^{102}\text{Sn}$ . The  $19/2^+$  and  $21/2^+$  states have the respective  $\pi g_{9/2}^{-1} \nu(d_{5/2}g_{7/2})_{6^+}$  and  $\pi g_{9/2}^{-1} \nu(g_{7/2}^2)_{6^+}$  configurations. The large separation between the  $19/2^+$  and  $21/2^+$  states is of course attributed to the strong repulsion between the aligned  $\pi g_{9/2}^{-1}$  and  $\nu g_{7/2}$ . It is worth noting that if the correction  $\Delta k^{T=1}(\pi g_{9/2}^{-1} \nu g_{7/2})_{8^+} = 1$  MeV is not taken into account, the calculated  $21/2^+$  with  $\alpha = 0.2$  lies at only  $\sim 350$  keV above  $19/2^+$ .

When the pure  $T = 0$   $p$ - $n$  quadrupole interaction is adopted, the calculated second  $7^+$ ,  $9^+$ , and  $11^+$  states are  $\sim 100$  keV higher than the first  $8^+$ ,  $10^+$ , and  $12^+$  states in  $^{102}\text{In}$ , inconsistent with the experimental results indicated in Fig. 4. These provide a supplement for the dominating  $T = 1$  channel  $p$ - $n$  interaction. In addition, the large level spacing between the  $12_1^+$  and  $11_2^+$  states is very similar to the large separation between the  $21/2^+$  and  $19/2^+$  states in  $^{101}\text{In}$  (see Fig. 4); the corresponding intrinsic structures as a matter of fact are somewhat alike (see Table I).

##### B. Level structure of positive-parity states in $^{99-101}\text{Cd}$

In the low-energy region of  $^{99}\text{Cd}$  [1], one may hope to find single-neutron states, i.e.,  $\nu d_{5/2}$  and  $\nu g_{7/2}$ . A large pairing energy gap comes following the single-neutron states. Thus, the levels above  $7/2^+$  should be the broken-pairing excitations

TABLE I. Structure of yrast and near yrast states in  $^{101-102}\text{In}$ . The leading component of configurations  $(p^{-1})_{J_p}^{\pi} (n^{2-3})_{J_n}^{\pi}$  and its squared amplitude (in percent) are tabulated in the third and second columns, where the superscript  $\pi$  in  $(p^{-1})_{J_p}^{\pi} (n^{2-3})_{J_n}^{\pi}$  means the parity of the one proton hole and 2-3 neutron subsystems. Expectation values of proton number  $\langle n_p \rangle$  (neutron number  $\langle n_n \rangle$ ) in two proton orbitals (in five neutron orbitals) are tabulated in the fourth and fifth columns (in the sixth through tenth columns).

$J_i^{\pi}$	leading config.		proton $\langle n_p \rangle$		neutron $\langle n_n \rangle$				
	%	$(p^{-1})_{J_p}^{\pi} (n^{2-3})_{J_n}^{\pi}$	$p_{1/2}^{-1}$	$g_{9/2}^{-1}$	$d_{5/2}$	$s_{1/2}$	$d_{3/2}$	$g_{7/2}$	$h_{11/2}$
$9/2^+$	83.32	$(p^{-1})_{9/2}^+(n^2)_0^+$	0.0	1.0	1.1	0.1	0.1	0.7	0.0
$13/2^+$	76.43	$(p^{-1})_{9/2}^+(n^2)_2^+$	0.0	1.0	1.5	0.0	0.0	0.4	0.0
$17/2^+$	97.54	$(p^{-1})_{9/2}^+(n^2)_6^+$	0.0	1.0	1.0	0.0	0.0	1.0	0.0
$19/2^+$	87.24	$(p^{-1})_{9/2}^+(n^2)_6^+$	0.0	1.0	1.0	0.0	0.0	1.0	0.0
$21/2^+$	100.0	$(p^{-1})_{9/2}^+(n^2)_6^+$	0.0	1.0	0.2	0.0	0.0	1.8	0.0
$6^+$	49.15	$(p^{-1})_{9/2}^+(n^3)_{7/2}^+$	0.0	1.0	1.7	0.1	0.1	1.1	0.0
$7_1^+$	47.85	$(p^{-1})_{9/2}^+(n^3)_{5/2}^+$	0.0	1.0	1.7	0.1	0.1	1.1	0.0
$7_2^+$	45.18	$(p^{-1})_{9/2}^+(n^3)_{7/2}^+$	0.0	1.0	1.7	0.1	0.1	1.1	0.0
$8^+$	48.92	$(p^{-1})_{9/2}^+(n^3)_{7/2}^+$	0.0	1.0	1.5	0.1	0.1	1.3	0.0
$9_1^+$	51.59	$(p^{-1})_{9/2}^+(n^3)_{11/2}^+$	0.0	1.0	1.9	0.0	0.0	1.0	0.0
$9_2^+$	31.40	$(p^{-1})_{9/2}^+(n^3)_{13/2}^+$	0.0	1.0	1.8	0.0	0.0	1.1	0.0
$10_1^+$	78.59	$(p^{-1})_{9/2}^+(n^3)_{15/2}^+$	0.0	1.0	1.9	0.0	0.0	1.0	0.0
$10_2^+$	61.56	$(p^{-1})_{9/2}^+(n^3)_{17/2}^+$	0.0	1.0	1.1	0.0	0.0	1.9	0.0
$11_1^+$	85.18	$(p^{-1})_{9/2}^+(n^3)_{15/2}^+$	0.0	1.0	2.0	0.0	0.0	1.0	0.0
$11_2^+$	72.89	$(p^{-1})_{9/2}^+(n^3)_{17/2}^+$	0.0	1.0	2.0	0.0	0.0	1.0	0.0
$12_1^+$	88.52	$(p^{-1})_{9/2}^+(n^3)_{17/2}^+$	0.0	1.0	1.1	0.0	0.0	1.9	0.0
$12_2^+$	94.02	$(p^{-1})_{9/2}^+(n^3)_{15/2}^+$	0.0	1.0	1.0	0.0	0.0	2.0	0.0
$13^+$	100.0	$(p^{-1})_{9/2}^+(n^3)_{17/2}^+$	0.0	1.0	1.0	0.0	0.0	2.0	0.0

TABLE II. Structure of yrast and near yrast states in  $^{99-101}\text{Cd}$ , tabulated in the same manner as Table I.

$J_i^\pi$	leading config.		proton $\langle n_a \rangle_p$		neutron $\langle n_a \rangle_n$				
	%	$(p^{-2})_{J_p}^+(n^{1-3})_{J_n}^\pi$	$p_{1/2}^{-1}$	$g_{9/2}^{-1}$	$d_{5/2}$	$s_{1/2}$	$d_{3/2}$	$g_{7/2}$	$h_{11/2}$
5/2 <sup>+</sup>	89.53	$(p^{-2})_0^+(n^1)_{5/2}^+$	0.1	1.9	1.0	0.0	0.0	0.0	0.0
7/2 <sup>+</sup>	84.59	$(p^{-2})_0^+(n^1)_{7/2}^+$	0.1	1.9	0.0	0.0	0.0	1.0	0.0
9/2 <sup>+</sup>	88.27	$(p^{-2})_2^+(n^1)_{5/2}^+$	0.0	2.0	1.0	0.0	0.0	0.0	0.0
11/2 <sup>+</sup>	79.30	$(p^{-2})_2^+(n^1)_{7/2}^+$	0.0	2.0	0.0	0.0	0.0	1.0	0.0
13/2 <sup>+</sup>	90.32	$(p^{-2})_4^+(n^1)_{5/2}^+$	0.0	2.0	1.0	0.0	0.0	0.0	0.0
17/2 <sup>+</sup>	91.73	$(p^{-2})_8^+(n^1)_{5/2}^+$	0.0	2.0	0.9	0.0	0.0	0.0	0.0
19/2 <sub>1</sub> <sup>+</sup>	95.20	$(p^{-2})_8^+(n^1)_{5/2}^+$	0.0	2.0	1.0	0.0	0.0	0.0	0.0
19/2 <sub>2</sub> <sup>+</sup>	81.28	$(p^{-2})_8^+(n^1)_{7/2}^+$	0.0	2.0	0.0	0.0	0.0	1.0	0.0
21/2 <sub>1</sub> <sup>+</sup>	96.71	$(p^{-2})_8^+(n^1)_{5/2}^+$	0.0	2.0	1.0	0.0	0.0	0.0	0.0
21/2 <sub>2</sub> <sup>+</sup>	96.71	$(p^{-2})_8^+(n^1)_{7/2}^+$	0.0	2.0	0.0	0.0	0.0	1.0	0.0
23/2 <sup>+</sup>	100.0	$(p^{-2})_8^+(n^1)_{7/2}^+$	0.0	2.0	0.0	0.0	0.0	1.0	0.0
0 <sup>+</sup>	82.06	$(p^{-2})_0^+(n^2)_{0}^+$	0.1	1.9	1.2	0.1	0.1	0.6	0.0
2 <sup>+</sup>	42.22	$(p^{-2})_2^+(n^2)_{0}^+$	0.0	2.0	1.2	0.2	0.1	0.5	0.0
4 <sub>1</sub> <sup>+</sup>	38.94	$(p^{-2})_0^+(n^2)_{4}^+$	0.0	2.0	1.4	0.1	0.1	0.4	0.0
4 <sub>2</sub> <sup>+</sup>	62.30	$(p^{-2})_0^+(n^2)_{4}^+$	0.1	1.9	1.5	0.0	0.1	0.4	0.0
6 <sub>1</sub> <sup>+</sup>	69.63	$(p^{-2})_0^+(n^2)_{6}^+$	0.1	1.9	1.0	0.0	0.0	1.0	0.0
6 <sub>2</sub> <sup>+</sup>	71.12	$(p^{-2})_6^+(n^2)_{0}^+$	0.0	2.0	1.3	0.1	0.1	1.5	0.0
8 <sub>1</sub> <sup>+</sup>	77.55	$(p^{-2})_8^+(n^2)_{0}^+$	0.0	2.0	1.2	0.1	0.1	0.6	0.0
8 <sub>2</sub> <sup>+</sup>	72.42	$(p^{-2})_2^+(n^2)_{6}^+$	0.0	2.0	1.0	0.0	0.0	1.0	0.0
10 <sup>+</sup>	84.75	$(p^{-2})_8^+(n^2)_{4}^+$	0.0	2.0	1.8	0.0	0.0	0.1	0.0
11 <sup>+</sup>	76.72	$(p^{-2})_8^+(n^2)_{6}^+$	0.0	2.0	1.0	0.0	0.0	1.0	0.0
12 <sup>+</sup>	74.57	$(p^{-2})_8^+(n^2)_{6}^+$	0.0	2.0	1.0	0.0	0.0	1.0	0.0
14 <sup>+</sup>	100.0	$(p^{-2})_8^+(n^2)_{6}^+$	0.0	2.0	1.0	0.0	0.0	1.0	0.0
5/2 <sup>+</sup>	73.39	$(p^{-2})_0^+(n^3)_{5/2}^+$	0.1	1.9	1.8	0.1	0.2	0.9	0.0
7/2 <sup>+</sup>	65.00	$(p^{-2})_0^+(n^3)_{7/2}^+$	0.1	1.9	1.5	0.2	0.1	1.2	0.0
9/2 <sup>+</sup>	39.99	$(p^{-2})_0^+(n^3)_{9/2}^+$	0.0	2.0	1.9	0.1	0.2	0.8	0.0
11/2 <sup>+</sup>	40.83	$(p^{-2})_2^+(n^3)_{7/2}^+$	0.0	2.0	1.6	0.2	0.1	1.1	0.0
13/2 <sup>+</sup>	41.04	$(p^{-2})_0^+(n^3)_{13/2}^+$	0.0	2.0	1.4	0.1	0.1	1.3	0.0
15/2 <sub>1</sub> <sup>+</sup>	44.08	$(p^{-2})_0^+(n^3)_{15/2}^+$	0.1	1.9	1.8	0.1	0.1	1.0	0.0
15/2 <sub>2</sub> <sup>+</sup>	31.82	$(p^{-2})_4^+(n^3)_{7/2}^+$	0.0	2.0	1.4	0.1	0.1	1.4	0.0
17/2 <sup>+</sup>	52.32	$(p^{-2})_0^+(n^3)_{17/2}^+$	0.1	1.9	1.0	0.0	0.1	1.9	0.0
19/2 <sub>1</sub> <sup>+</sup>	54.23	$(p^{-2})_8^+(n^3)_{5/2}^+$	0.0	2.0	2.0	0.1	0.1	0.7	0.0
19/2 <sub>2</sub> <sup>+</sup>	61.71	$(p^{-2})_8^+(n^3)_{7/2}^+$	0.0	2.0	1.7	0.1	0.1	1.1	0.0
21/2 <sup>+</sup>	76.35	$(p^{-2})_8^+(n^3)_{5/2}^+$	0.0	2.0	2.1	0.1	0.1	0.7	0.0
23/2 <sub>1</sub> <sup>+</sup>	44.62	$(p^{-2})_8^+(n^3)_{9/2}^+$	0.0	2.0	1.8	0.0	0.1	1.1	0.0
23/2 <sub>2</sub> <sup>+</sup>	46.59	$(p^{-2})_8^+(n^3)_{11/2}^+$	0.0	2.0	1.6	0.1	0.1	1.2	0.0
25/2 <sub>1</sub> <sup>+</sup>	37.91	$(p^{-2})_6^+(n^3)_{15/2}^+$	0.0	2.0	2.1	0.0	0.0	0.8	0.0
25/2 <sub>2</sub> <sup>+</sup>	70.78	$(p^{-2})_8^+(n^3)_{9/2}^+$	0.0	2.0	2.5	0.0	0.0	0.4	0.0
27/2 <sub>1</sub> <sup>+</sup>	53.08	$(p^{-2})_8^+(n^3)_{15/2}^+$	0.0	2.0	1.9	0.0	0.0	1.0	0.0

coupled to the single-neutron states. Such  $\pi g_{9/2}^{-2} \nu(d_{5/2}, g_{7/2})$  structure persists till the stretched coupled  $23/2^+$  level. Shell model calculations provide an explicit explanation to the first and second  $19/2^+$  and  $21/2^+$  states resulting from the  $\nu d_{5/2}$  and  $\nu g_{7/2}$  orbitals, exhibited in Table II. The large separation between the first fully aligned  $21/2^+$  and  $23/2^+$  states, having a resemblance to that between the  $19/2^+$  and  $21/2^+$  states in  $^{101}\text{In}$ , gives a hint of the enhanced  $T = 1$  channel  $p$ - $n$  interaction.

The level structure of  $^{100}\text{Cd}$  [3,23] can be classified according to active nucleon number. The  $2^+ - 8_1^+$  states belong to the two-particle states. Inspection of the wave function accounts for the neutron nature of the first  $6^+$  state, while the intrinsic

structure of the second  $6^+$  state has more resemblance to the first  $8^+$  state which is the dominating proton configuration. The four-particle structure in  $^{100}\text{Cd}$  is preserved up to the maximum spin 14 generated from two  $g_{9/2}$  proton holes together with two neutrons in  $\nu(d_{5/2}, g_{7/2})$ . Again, there is a large energy gap below the stretched coupled  $14^+$  state coming from the strong  $T = 1$  dominated  $p$ - $n$  repulsion between the aligned  $\pi g_{9/2}^{-1}$  and  $\nu g_{7/2}$ .

Odd- $A$  nuclei usually exhibit level structures with spin sequences and energy spacings similar to those of the yrast level schemes of adjacent even-even cores. As shown in Fig. 5, the energy spacings of the  $5/2^+$  ( $7/2^+$ ),  $9/2^+$  ( $11/2^+$ ),  $13/2^+$  ( $15/2_1^+$ ),  $17/2^+$  ( $19/2^+$ ), and  $21/2_1^+$  levels are similar to

TABLE III. Structure of yrast and near yrast states in  $^{98-100}\text{Ag}$ , tabulated in the same manner as Table I.

$J_i^\pi$	leading config.		proton $\langle n_a \rangle_p$		neutron $\langle n_a \rangle_n$				
	%	$(p^{-3})_{J_p}^\pi (n^{1-3})_{J_n}^\pi$	$p_{1/2}^{-1}$	$g_{9/2}^{-1}$	$d_{5/2}$	$s_{1/2}$	$d_{3/2}$	$g_{7/2}$	$h_{11/2}$
5 <sup>+</sup>	84.63	$(p^{-3})_{9/2}^+(n^1)_{5/2}^+$	0.1	2.9	1.0	0.0	0.0	0.0	0.0
6 <sup>+</sup>	83.23	$(p^{-3})_{9/2}^+(n^1)_{5/2}^+$	0.1	2.9	1.0	0.0	0.0	0.0	0.0
7 <sup>+</sup>	89.10	$(p^{-3})_{9/2}^+(n^1)_{5/2}^+$	0.1	2.9	1.0	0.0	0.0	0.0	0.0
8 <sup>+</sup>	84.31	$(p^{-3})_{9/2}^+(n^1)_{7/2}^+$	0.1	2.9	0.0	0.0	0.0	0.9	0.0
9 <sup>+</sup>	89.03	$(p^{-3})_{13/2}^+(n^1)_{5/2}^+$	0.0	3.0	1.0	0.0	0.0	0.0	0.0
10 <sup>+</sup>	52.08	$(p^{-3})_{17/2}^+(n^1)_{5/2}^+$	0.0	3.0	0.7	0.0	0.0	0.3	0.0
11 <sup>+</sup>	73.64	$(p^{-3})_{17/2}^+(n^1)_{5/2}^+$	0.0	3.0	1.0	0.0	0.0	0.0	0.0
12 <sup>+</sup>	97.88	$(p^{-3})_{21/2}^+(n^1)_{5/2}^+$	0.0	3.0	1.0	0.0	0.0	0.0	0.0
13 <sub>1</sub> <sup>+</sup>	97.93	$(p^{-3})_{21/2}^+(n^1)_{5/2}^+$	0.0	3.0	1.0	0.0	0.0	0.0	0.0
13 <sub>2</sub> <sup>+</sup>	97.93	$(p^{-3})_{21/2}^+(n^1)_{7/2}^+$	0.0	3.0	0.0	0.0	0.0	1.0	0.0
14 <sup>+</sup>	100.0	$(p^{-3})_{21/2}^+(n^1)_{7/2}^+$	0.0	3.0	0.0	0.0	0.0	1.0	0.0
9/2 <sup>+</sup>	74.35	$(p^{-3})_{9/2}^+(n^2)_0^+$	0.1	2.9	1.2	0.1	0.1	0.5	0.0
13/2 <sup>+</sup>	45.88	$(p^{-3})_{9/2}^+(n^2)_2^+$	0.0	3.0	1.4	0.1	0.1	0.4	0.0
17/2 <sup>+</sup>	31.14	$(p^{-3})_{9/2}^+(n^2)_6^+$	0.1	2.9	1.2	0.1	0.1	0.6	0.0
19/2 <sup>+</sup>	69.28	$(p^{-3})_{9/2}^+(n^2)_6^+$	0.1	2.9	1.0	0.0	0.0	1.0	0.0
21/2 <sub>1</sub> <sup>+</sup>	59.12	$(p^{-3})_{9/2}^+(n^2)_6^+$	0.1	2.9	1.1	0.0	0.1	0.8	0.0
21/2 <sub>2</sub> <sup>+</sup>	66.89	$(p^{-3})_{21/2}^+(n^2)_0^+$	0.0	3.0	1.3	0.1	0.1	0.5	0.0
23/2 <sup>+</sup>	50.97	$(p^{-3})_{13/2}^+(n^2)_6^+$	0.0	3.0	1.0	0.0	0.0	1.0	0.0
25/2 <sup>+</sup>	39.56	$(p^{-3})_{13/2}^+(n^2)_6^+$	0.0	3.0	1.4	0.0	0.0	0.6	0.0
27/2 <sup>+</sup>	43.56	$(p^{-3})_{17/2}^+(n^2)_6^+$	0.0	3.0	1.0	0.0	0.0	1.0	0.0
29/2 <sub>1</sub> <sup>+</sup>	91.96	$(p^{-3})_{21/2}^+(n^2)_4^+$	0.0	3.0	1.9	0.0	0.0	0.1	0.0
29/2 <sub>2</sub> <sup>+</sup>	58.67	$(p^{-3})_{21/2}^+(n^2)_6^+$	0.0	3.0	1.0	0.0	0.0	1.0	0.0
31/2 <sub>1</sub> <sup>+</sup>	98.10	$(p^{-3})_{21/2}^+(n^2)_6^+$	0.0	3.0	1.0	0.0	0.0	1.0	0.0
31/2 <sub>2</sub> <sup>+</sup>	97.54	$(p^{-3})_{21/2}^+(n^2)_5^+$	0.0	3.0	1.0	0.0	0.0	1.0	0.0
33/2 <sup>+</sup>	100.0	$(p^{-3})_{21/2}^+(n^2)_6^+$	0.0	3.0	1.0	0.0	0.0	1.0	0.0
5 <sup>+</sup>	26.39	$(p^{-3})_{7/2}^+(n^3)_{3/2}^+$	0.0	3.0	2.0	0.2	0.2	0.6	0.0
6 <sup>+</sup>	21.36	$(p^{-3})_{9/2}^+(n^3)_{3/2}^+$	0.0	3.0	1.8	0.2	0.2	0.8	0.0
7 <sub>1</sub> <sup>+</sup>	47.97	$(p^{-3})_{9/2}^+(n^3)_{7/2}^+$	0.1	2.9	1.7	0.2	0.1	1.0	0.0
7 <sub>2</sub> <sup>+</sup>	56.25	$(p^{-3})_{9/2}^+(n^3)_{5/2}^+$	0.1	2.9	2.0	0.1	0.2	0.7	0.0
8 <sub>1</sub> <sup>+</sup>	48.25	$(p^{-3})_{9/2}^+(n^3)_{7/2}^+$	0.1	2.9	1.6	0.2	0.1	1.1	0.0
8 <sub>2</sub> <sup>+</sup>	17.38	$(p^{-3})_{9/2}^+(n^3)_{9/2}^+$	0.0	3.0	1.7	0.2	0.2	0.9	0.0
9 <sub>1</sub> <sup>+</sup>	35.72	$(p^{-3})_{9/2}^+(n^3)_{11/2}^+$	0.0	3.0	1.7	0.2	0.1	1.0	0.0
9 <sub>2</sub> <sup>+</sup>	31.91	$(p^{-3})_{9/2}^+(n^3)_{9/2}^+$	0.0	3.0	2.0	0.1	0.1	0.7	0.0
10 <sub>1</sub> <sup>+</sup>	35.44	$(p^{-3})_{9/2}^+(n^3)_{11/2}^+$	0.0	3.0	1.7	0.1	0.1	1.1	0.0
10 <sub>2</sub> <sup>+</sup>	22.99	$(p^{-3})_{9/2}^+(n^3)_{13/2}^+$	0.1	2.9	1.6	0.1	0.1	1.2	0.0
11 <sup>+</sup>	45.98	$(p^{-3})_{9/2}^+(n^3)_{15/2}^+$	0.1	2.9	1.9	0.1	0.1	0.9	0.0
12 <sup>+</sup>	47.72	$(p^{-3})_{9/2}^+(n^3)_{15/2}^+$	0.0	3.0	1.9	0.1	0.1	0.9	0.0
13 <sub>1</sub> <sup>+</sup>	78.19	$(p^{-3})_{21/2}^+(n^3)_{5/2}^+$	0.0	3.0	2.2	0.1	0.1	0.6	0.0
13 <sub>2</sub> <sup>+</sup>	34.37	$(p^{-3})_{9/2}^+(n^3)_{17/2}^+$	0.0	3.0	1.3	0.0	0.1	1.5	0.0
14 <sup>+</sup>	40.31	$(p^{-3})_{13/2}^+(n^3)_{15/2}^+$	0.0	3.0	1.9	0.1	0.0	1.0	0.0
15 <sup>+</sup>	21.56	$(p^{-3})_{17/2}^+(n^3)_{13/2}^+$	0.0	3.0	1.8	0.0	0.0	1.2	0.0
8 <sup>-</sup>	43.28	$(p^{-3})_{9/2}^+(n^3)_{11/2}^-$	0.0	3.0	1.0	0.2	0.2	0.6	1.0
9 <sub>1</sub> <sup>-</sup>	57.38	$(p^{-3})_{9/2}^+(n^3)_{11/2}^-$	0.1	2.9	1.0	0.2	0.2	0.6	1.0
9 <sub>2</sub> <sup>-</sup>	69.92	$(p^{-3})_{17/2}^+(n^3)_{7/2}^-$	1.0	2.0	1.6	0.1	0.1	1.2	0.0
10 <sub>1</sub> <sup>-</sup>	51.59	$(p^{-3})_{17/2}^+(n^3)_{5/2}^-$	1.0	2.0	2.0	0.1	0.1	0.7	0.0
10 <sub>2</sub> <sup>-</sup>	56.48	$(p^{-3})_{9/2}^+(n^3)_{11/2}^-$	0.1	2.9	1.1	0.2	0.2	0.5	1.0
11 <sup>-</sup>	64.03	$(p^{-3})_{17/2}^+(n^3)_{5/2}^-$	1.0	2.0	2.0	0.1	0.1	0.8	0.0
12 <sup>-</sup>	35.10	$(p^{-3})_{9/2}^+(n^3)_{15/2}^-$	0.0	3.0	1.2	0.1	0.2	0.5	1.0
13 <sup>-</sup>	50.12	$(p^{-3})_{9/2}^+(n^3)_{21/2}^-$	0.1	2.9	0.9	0.0	0.1	1.0	1.0
14 <sub>1</sub> <sup>-</sup>	63.79	$(p^{-3})_{9/2}^+(n^3)_{21/2}^-$	0.1	2.9	0.9	0.0	0.0	1.0	1.0
14 <sub>2</sub> <sup>-</sup>	45.98	$(p^{-3})_{9/2}^+(n^3)_{23/2}^-$	0.1	2.9	0.9	0.1	0.1	0.9	1.0
15 <sup>-</sup>	41.69	$(p^{-3})_{9/2}^+(n^3)_{23/2}^-$	0.1	2.9	0.9	0.0	0.0	1.0	1.0
16 <sub>1</sub> <sup>-</sup>	43.67	$(p^{-3})_{13/2}^+(n^3)_{21/2}^-$	0.0	3.0	1.0	0.0	0.0	1.0	1.0
16 <sub>2</sub> <sup>-</sup>	39.19	$(p^{-3})_{9/2}^+(n^3)_{23/2}^-$	0.0	3.0	1.0	0.1	0.1	0.8	1.0

TABLE III. (Continued)

$J_i^\pi$	leading config.		proton $\langle n_a \rangle_p$		neutron $\langle n_a \rangle_n$				
	%	$(p^{-3})_{J_p}^\pi (n^{1-3})_{J_n}^\pi$	$p_{1/2}^{-1}$	$g_{9/2}^{-1}$	$d_{5/2}$	$s_{1/2}$	$d_{3/2}$	$g_{7/2}$	$h_{11/2}$
$17^-$	63.24	$(p^{-3})_{13/2}^+ (n^3)_{21/2}^-$	0.0	3.0	1.0	0.0	0.0	1.0	1.0
$18^-$	41.53	$(p^{-3})_{17/2}^+ (n^3)_{21/2}^-$	0.0	3.0	1.0	0.0	0.0	1.0	1.0

those of the  $0^+$ ,  $2^+$ ,  $4_1^+$ ,  $6_1^+$ , and  $8_1^+$  states in the  $^{100}\text{Cd}$  core nucleus; the weak-coupling behaviors are further supported somewhat by the corresponding wave function components in Table II except for the  $19/2^+$  where two  $g_{9/2}$  proton holes couple to 8 rather than 6. We can see from Table II that the  $23/2^+ - 27/2^+$  states belong to the five-particle structure. Thus, the expected three-particle exhausted  $(\pi g_{9/2}^{-2} \nu g_{7/2})_{23/2^+}$  state does not emerge in  $^{101}\text{Cd}$  according to the calculated results. This may be because the dominated  $T = 1$  channel  $p$ - $n$  interaction between the aligned  $\pi g_{9/2}^{-1}$  and  $\nu g_{7/2}$  strongly repulses with each other and leads to a  $23/2^+$  state much higher in energy.

### C. Level structure of positive-parity states in $^{98-100}\text{Ag}$

The  $\pi g_{9/2}^{-1} \nu d_{5/2}$  particle-hole interaction favors  $J_{\max} - 2 = 5$  for the ground state differing from the experimental ground state  $6^+$  in  $^{98}\text{Ag}$ . The jumping of a neutron into the  $g_{7/2}$  orbital to form the aligned  $8^+$  needs more energy due to the monopole correlations and the strong repulsion between the aligned  $\pi g_{9/2}^{-1}$  and  $\nu g_{7/2}$ . This leads to a large energy gap below the  $8^+$  state. The levels above concern  $\pi g_{9/2}^{-3} \nu (d_{5/2}, g_{7/2})$  excitations. Also, the topmost stretched coupled  $14^+$  state is much higher in energy.

The excited state  $13/2^+$  in  $^{99}\text{Ag}$  [6] can be described by angular momentum coupling of  $\pi g_{9/2}^{-1}$  with the core  $2^+$  state, and the  $17/2^+ - 21/2_1^+$  states correspond to the multiplet of  $\pi g_{9/2}^{-1} \otimes \nu (d_{5/2} g_{7/2})_{6^+}$ , where the fully aligned  $21/2_1^+$  state is separated from its multiplet members. The  $21/2_2^+$  state is constructed by exhausted three proton holes with one neutron pair in  $\nu d_{5/2}$  coupling to spin zero. The main components of the  $23/2^+ - 27/2^+$  states consist of an odd proton hole and a proton pair coupling to  $2^+$  or  $4^+$  in the  $\pi g_{9/2}$  orbital and a neutron pair in  $\nu (d_{5/2}, g_{7/2})$  orbitals coupling to  $6^+$ . The dominating proton configurations for  $29/2^+ - 33/2^+$  states is  $\pi (g_{9/2}^{-3})_{21/2^+}$  while two neutrons occupying the  $\nu d_{5/2}$  and  $\nu g_{7/2}$  couple to spins 4–6.

Four energy gaps are observed in  $^{100}\text{Ag}$  [7] (see Fig. 6). The first two gaps can be approximately regarded as the corresponding  $0^+ - 2^+$  and  $2^+ - 4^+$  level spacings in  $^{100}\text{Cd}$  according to the weak-coupling behaviors. The last one is due to the excitation from a four-particle to six-particle state, which needs more energy. The third gap might be induced by the stretched coupled four-particle excitations, where the  $12^+$ ,  $13_1^+$ , and  $13_2^+$  states might have the main components:  $\pi g_{9/2}^{-1} \otimes \nu (d_{5/2}^2)_{4^+} \otimes \nu g_{7/2}$ ,  $\pi (g_{9/2}^{-3})_{21/2^+} \otimes \nu d_{5/2}$ , and  $\pi g_{9/2}^{-1} \otimes \nu d_{5/2} \otimes \nu (g_{7/2}^2)_{6^+}$  (see Table III), respectively.

### D. Level structure of positive-parity states in $^{97-99}\text{Pd}$

Only two members of high-spin states up to  $25^+$  in  $^{97}\text{Pd}$  [8] concern the  $\nu g_{7/2}$  excitation. The energy for  $5/2^+ \rightarrow 7/2^+$  excitation can be approximately regarded as the sum of the  $\nu g_{7/2}$  single-particle excitation energy, the monopole correlations, and the  $p$ - $n$  interaction. Given a cursory glance at the needed energy, it may be seen that the  $5/2^+ \rightarrow 7/2^+$  excitation is a very close approximation to  $[(\pi g_{9/2}^{-2})_{8^+} \otimes \nu d_{5/2}]_{21/2^+} \rightarrow [(\pi g_{9/2}^{-2})_{8^+} \otimes \nu g_{7/2}]_{23/2^+}$  if the  $8^+$  state is only a spectator. However, the  $21/2^+ - 23/2^+$  level spacing is much larger than that between  $5/2^+$  and  $7/2^+$ . This difference naturally comes from the  $p$ - $n$  interaction. We use  $\alpha = 0.425$  and  $\Delta k^{T=1} (\pi g_{9/2}^{-1} \nu g_{7/2})_{8^+} = 0.25$  MeV to improve such difference.

The energy gap coming above the fully aligned two-proton  $8^+$  state in  $^{98}\text{Pd}$  [9] is due to the level structure evolving from the two-particle to four-particle state. The fully aligned four-particle state  $[(\pi g_{9/2}^{-2})_{8^+} (\nu d_{5/2} g_{7/2})_{6^+}]_{14_1^+}$  is far away from four-particle state  $[(\pi g_{9/2}^{-2})_{8^+} \nu (d_{5/2}, g_{7/2})_{4^+}]_{12_2^+}$  and very close to six-particle state  $[(\pi g_{9/2}^{-4})_{10^+} (\nu d_{5/2}^2)_{4^+}]_{14_2^+}$  (see Table IV). Note that the  $14_1^+ - 12_2^+$  level spacing is larger than that between  $6^+$  and  $4^+$  states due to the strong  $p$ - $n$  repulsion between the aligned  $\pi g_{9/2}^{-1}$  and  $\nu g_{7/2}$ . The energy gap between  $14_2^+$  ( $16_2^+$ ) and  $15_1^+$  ( $18^+$ ) is attributed to the neutron  $4^+ \rightarrow 6^+$  excitation.

The leading configuration of the ground state in  $^{99}\text{Pd}$  is two  $g_{9/2}$  proton-hole pairs, two  $d_{5/2}$  neutrons paired to angular momentum zero, and a  $d_{5/2}$  odd neutron. The  $7/2^+$  level can be an excitation of the odd neutron to the  $g_{7/2}$  orbital. The energy spacings of the  $5/2^+ - 19/2^+$  in  $^{99}\text{Pd}$  are somewhat similar to those of the  $0^+ - 6^+$  states in the  $^{98}\text{Pd}$  [9] core nucleus (see Fig. 7). In fact, Table IV shows that the  $5/2^+$  ( $7/2^+$ ),  $9/2^+$  ( $11/2^+$ ),  $13/2^+$  ( $15/2_1^+$ ), and  $17/2_2^+$  ( $19/2^+$ ) levels can be approximately regarded as the coupling of the  $\nu d_{5/2}$  ( $\nu g_{7/2}$ ) proton to the  $0^+$ ,  $2^+$ ,  $4^+$ , and  $6^+$  states of the core nucleus  $^{98}\text{Pd}$ . The maximum spin that can be reached by the two proton holes in the  $g_{9/2}$  orbital along with the one neutron in the  $g_{7/2}$  orbital is  $23/2$ . The experimentally observed three-particle  $23/2^+$  state intrudes into the energy region of five-particle  $25/2^+ - 27/2^+$  states with probable configurations  $\pi (g_{9/2}^{-2})_{8^+} \otimes \nu (d_{5/2}^2)_{2^+} \otimes \nu (d_{5/2}, g_{7/2})$ . The  $29/2^+ - 33/2^+$  states might be  $\pi (g_{9/2}^{-2})_{8^+} \otimes \nu (d_{5/2} g_{7/2})_{4^+, 6^+}^2 \otimes \nu (d_{5/2}, g_{7/2})$  and the large level spacing between the  $27/2^+$  and  $29/2^+$  states therefore corresponds to  $2^+ \rightarrow 4^+$ ,  $6^+$  excitations in  $^{98}\text{Pd}$ , where the calculated excitation energy for the fully aligned five-particle  $33/2^+$  state is larger than the experimental one. The above excited states can be interpreted in terms of all the valence-nucleon excitations with respect to the doubly magic  $^{100}\text{Sn}$  core.

TABLE IV. Structure of yrast and near yrast states in  $^{97-99}\text{Pd}$ , tabulated in the same manner as Table I.

$J_i^\pi$	leading config.		proton $\langle n_a \rangle_p$		neutron $\langle n_a \rangle_n$				
	%	$(p^{-4})_p^\pi (n^{1-3})_n^\pi$	$p_{1/2}^{-1}$	$g_{9/2}^{-1}$	$d_{5/2}$	$s_{1/2}$	$d_{3/2}$	$g_{7/2}$	$h_{11/2}$
5/2 <sup>+</sup>	84.18	$(p^{-4})_0^+(n^1)_{5/2}^+$	0.2	3.8	1.0	0.0	0.0	0.0	0.0
7/2 <sup>+</sup>	78.88	$(p^{-4})_0^+(n^1)_{7/2}^+$	0.3	3.7	0.0	0.0	0.0	0.9	0.0
9/2 <sup>+</sup>	81.11	$(p^{-4})_2^+(n^1)_{5/2}^+$	0.1	3.9	0.9	0.0	0.0	0.0	0.0
13/2 <sup>+</sup>	76.57	$(p^{-4})_4^+(n^1)_{5/2}^+$	0.0	4.0	0.9	0.0	0.0	0.0	0.0
17/2 <sup>+</sup>	67.39	$(p^{-4})_6^+(n^1)_{5/2}^+$	0.1	3.9	1.0	0.0	0.0	0.0	0.0
19/2 <sup>+</sup>	85.09	$(p^{-4})_8^+(n^1)_{5/2}^+$	0.1	3.9	1.0	0.0	0.0	0.0	0.0
21/2 <sup>+</sup>	91.83	$(p^{-4})_8^+(n^1)_{5/2}^+$	0.1	3.9	1.0	0.0	0.0	0.0	0.0
23/2 <sup>+</sup>	88.36	$(p^{-4})_8^+(n^1)_{7/2}^+$	0.1	3.9	0.0	0.0	0.0	0.9	0.0
25/2 <sup>+</sup>	91.85	$(p^{-4})_{10}^+(n^1)_{5/2}^+$	0.0	4.0	1.0	0.0	0.0	0.0	0.0
0 <sup>+</sup>	76.03	$(p^{-4})_0^+(n^2)_0^+$	0.2	3.8	1.3	0.1	0.1	0.5	0.0
2 <sup>+</sup>	40.38	$(p^{-4})_2^+(n^2)_0^+$	0.2	3.8	1.3	0.2	0.2	0.3	0.0
4 <sup>+</sup>	29.07	$(p^{-4})_2^+(n^2)_2^+$	0.1	3.9	1.3	0.2	0.2	0.3	0.0
6 <sup>+</sup>	46.56	$(p^{-4})_0^+(n^2)_6^+$	0.2	3.8	1.0	0.1	0.1	0.8	0.0
8 <sup>+</sup>	70.63	$(p^{-4})_8^+(n^2)_0^+$	0.1	3.9	1.3	0.1	0.1	0.4	0.0
9 <sup>+</sup>	48.43	$(p^{-4})_8^+(n^2)_2^+$	0.0	4.0	1.4	0.2	0.1	0.3	0.0
10 <sub>1</sub> <sup>+</sup>	51.39	$(p^{-4})_8^+(n^2)_2^+$	0.0	4.0	1.5	0.1	0.1	0.3	0.0
10 <sub>2</sub> <sup>+</sup>	51.62	$(p^{-4})_4^+(n^2)_6^+$	0.0	4.0	1.1	0.0	0.1	0.8	0.0
10 <sub>3</sub> <sup>+</sup>	28.62	$(p^{-4})_6^+(n^2)_6^+$	0.1	3.9	1.2	0.0	0.1	0.7	0.0
11 <sup>+</sup>	54.36	$(p^{-4})_8^+(n^2)_4^+$	0.1	3.9	1.5	0.0	0.1	0.4	0.0
12 <sub>1</sub> <sup>+</sup>	42.70	$(p^{-4})_6^+(n^2)_6^+$	0.1	3.9	1.2	0.0	0.0	0.7	0.0
12 <sub>2</sub> <sup>+</sup>	34.79	$(p^{-4})_8^+(n^2)_4^+$	0.1	3.9	1.4	0.0	0.0	0.5	0.0
13 <sup>+</sup>	74.59	$(p^{-4})_8^+(n^2)_6^+$	0.1	3.9	1.0	0.0	0.0	1.0	0.0
14 <sub>1</sub> <sup>+</sup>	80.02	$(p^{-4})_8^+(n^2)_6^+$	0.1	3.9	1.0	0.0	0.0	0.9	0.0
14 <sub>2</sub> <sup>+</sup>	57.11	$(p^{-4})_{10}^+(n^2)_4^+$	0.0	4.0	1.8	0.0	0.0	0.1	0.0
15 <sub>1</sub> <sup>+</sup>	68.23	$(p^{-4})_{10}^+(n^2)_6^+$	0.0	4.0	1.0	0.0	0.0	1.0	0.0
15 <sub>2</sub> <sup>+</sup>	71.84	$(p^{-4})_{10}^+(n^2)_5^+$	0.0	4.0	1.1	0.0	0.0	0.9	0.0
16 <sub>1</sub> <sup>+</sup>	81.69	$(p^{-4})_{10}^+(n^2)_6^+$	0.0	4.0	1.0	0.0	0.0	0.9	0.0
16 <sub>2</sub> <sup>+</sup>	90.87	$(p^{-4})_{12}^+(n^2)_4^+$	0.0	4.0	1.9	0.0	0.0	0.1	0.0
17 <sup>+</sup>	99.89	$(p^{-4})_{12}^+(n^2)_6^+$	0.0	4.0	1.0	0.0	0.0	1.0	0.0
18 <sup>+</sup>	100.0	$(p^{-4})_{12}^+(n^2)_6^+$	0.0	4.0	1.0	0.0	0.0	1.0	0.0
5 <sup>-</sup>	70.53	$(p^{-4})_5^-(n^2)_0^+$	1.0	3.0	1.2	0.1	0.1	0.5	0.0
7 <sup>-</sup>	33.85	$(p^{-4})_5^-(n^2)_2^+$	1.0	3.0	1.3	0.1	0.1	0.4	0.0
9 <sup>-</sup>	23.91	$(p^{-4})_7^-(n^2)_2^+$	1.0	3.0	1.3	0.1	0.1	0.5	0.0
11 <sup>-</sup>	73.48	$(p^{-4})_{11}^-(n^2)_0^+$	1.0	3.0	1.3	0.1	0.1	0.5	0.0
12 <sup>-</sup>	52.20	$(p^{-4})_7^-(n^2)_6^+$	1.0	3.0	1.0	0.0	0.0	1.0	0.0
13 <sup>-</sup>	54.51	$(p^{-4})_{11}^-(n^2)_2^+$	1.0	3.0	1.5	0.0	0.0	0.4	0.0
5/2 <sup>+</sup>	63.82	$(p^{-4})_0^+(n^3)_{5/2}^+$	0.2	3.8	1.9	0.1	0.2	0.7	0.0
7/2 <sup>+</sup>	56.28	$(p^{-4})_0^+(n^3)_{7/2}^+$	0.2	3.8	1.6	0.2	0.1	1.1	0.0
9/2 <sup>+</sup>	33.25	$(p^{-4})_0^+(n^3)_{9/2}^+$	0.1	3.9	1.9	0.2	0.2	0.7	0.0
11/2 <sup>+</sup>	37.99	$(p^{-4})_2^+(n^3)_{7/2}^+$	0.1	3.9	1.6	0.2	0.2	1.0	0.0
13/2 <sup>+</sup>	26.05	$(p^{-4})_2^+(n^3)_{9/2}^+$	0.1	3.9	1.7	0.1	0.2	1.0	0.0
15/2 <sub>1</sub> <sup>+</sup>	31.08	$(p^{-4})_4^+(n^3)_{7/2}^+$	0.1	3.9	1.7	0.2	0.1	1.0	0.0
15/2 <sub>2</sub> <sup>+</sup>	23.51	$(p^{-4})_4^+(n^3)_{7/2}^+$	0.1	3.9	1.7	0.1	0.2	1.0	0.0
17/2 <sub>1</sub> <sup>+</sup>	19.54	$(p^{-4})_4^+(n^3)_{9/2}^+$	0.1	3.9	1.5	0.1	0.2	1.1	0.0
17/2 <sub>2</sub> <sup>+</sup>	37.76	$(p^{-4})_6^+(n^3)_{5/2}^+$	0.0	4.0	1.9	0.1	0.2	0.8	0.0
19/2 <sup>+</sup>	22.52	$(p^{-4})_4^+(n^3)_{11/2}^+$	0.0	4.0	1.6	0.2	0.1	1.0	0.0
21/2 <sub>1</sub> <sup>+</sup>	70.16	$(p^{-4})_8^+(n^3)_{5/2}^+$	0.1	3.9	2.2	0.1	0.1	0.5	0.0
21/2 <sub>2</sub> <sup>+</sup>	49.10	$(p^{-4})_8^+(n^3)_{7/2}^+$	0.1	3.9	1.6	0.1	0.1	1.2	0.0
23/2 <sup>+</sup>	44.81	$(p^{-4})_8^+(n^3)_{7/2}^+$	0.0	4.0	1.7	0.1	0.1	1.1	0.0
25/2 <sub>1</sub> <sup>+</sup>	35.07	$(p^{-4})_8^+(n^3)_{9/2}^+$	0.0	4.0	1.9	0.1	0.1	0.9	0.0
25/2 <sub>2</sub> <sup>+</sup>	34.30	$(p^{-4})_8^+(n^3)_{9/2}^+$	0.0	4.0	1.9	0.1	0.1	0.8	0.0
27/2 <sup>+</sup>	45.24	$(p^{-4})_8^+(n^3)_{11/2}^+$	0.0	4.0	1.8	0.1	0.1	1.0	0.0
29/2 <sub>1</sub> <sup>+</sup>	29.82	$(p^{-4})_8^+(n^3)_{13/2}^+$	0.1	3.9	1.7	0.1	0.1	1.1	0.0
29/2 <sub>2</sub> <sup>+</sup>	34.95	$(p^{-4})_8^+(n^3)_{15/2}^+$	0.1	3.9	1.5	0.0	0.1	1.4	0.0

TABLE IV. (Continued)

$J_i^\pi$	leading config.		proton $\langle n_a \rangle_p$		neutron $\langle n_a \rangle_n$				
	%	$(p^{-4})_p^\pi (n^{1-3})_{J_n}^\pi$	$p_{1/2}^{-1}$	$g_{9/2}^{-1}$	$d_{5/2}$	$s_{1/2}$	$d_{3/2}$	$g_{7/2}$	$h_{11/2}$
31/2 <sup>+</sup>	65.60	$(p^{-4})_8^+(n^3)_{15/2}^+$	0.1	3.9	1.9	0.0	0.0	1.0	0.0
33/2 <sup>+</sup>	65.47	$(p^{-4})_8^+(n^3)_{17/2}^+$	0.1	3.9	1.1	0.0	0.1	1.8	0.0
35/2 <sup>+</sup>	74.29	$(p^{-4})_{10}^+(n^3)_{15/2}^+$	0.0	4.0	1.9	0.0	0.0	1.0	0.0
37/2 <sup>+</sup>	73.72	$(p^{-4})_{10}^+(n^3)_{17/2}^+$	0.0	4.0	1.1	0.0	0.0	1.9	0.0
37/2 <sup>+</sup>	88.02	$(p^{-4})_{12}^+(n^3)_{15/2}^+$	0.0	4.0	1.9	0.0	0.0	1.0	0.0
39/2 <sup>+</sup>	99.98	$(p^{-4})_{12}^+(n^3)_{15/2}^+$	0.0	4.0	2.0	0.0	0.0	1.0	0.0
11/2 <sup>-</sup>	60.31	$(p^{-4})_6^+(n^3)_{11/2}^-$	0.2	3.8	1.0	0.2	0.2	0.6	1.0
15/2 <sup>-</sup>	46.11	$(p^{-4})_5^-(n^3)_{7/2}^+$	1.0	3.0	1.6	0.2	0.1	1.1	0.0
19/2 <sup>-</sup>	30.53	$(p^{-4})_5^-(n^3)_{11/2}^-$	1.0	3.0	1.7	0.2	0.1	1.0	0.0
23/2 <sup>-</sup>	27.82	$(p^{-4})_6^+(n^3)_{11/2}^-$	0.1	3.9	1.0	0.2	0.2	0.6	1.0
27/2 <sup>-</sup>	46.67	$(p^{-4})_8^+(n^3)_{11/2}^-$	0.0	4.0	1.2	0.1	0.2	0.5	1.0
31/2 <sup>-</sup>	34.29	$(p^{-4})_8^+(n^3)_{15/2}^-$	0.0	4.0	1.2	0.1	0.1	0.6	1.0
35/2 <sup>-</sup>	58.91	$(p^{-4})_8^+(n^3)_{21/2}^-$	0.1	3.9	1.0	0.0	0.0	1.0	1.0
39/2 <sup>-</sup>	61.27	$(p^{-4})_8^+(n^3)_{23/2}^-$	0.0	4.0	1.0	0.1	0.0	0.9	1.0
43/2 <sup>-</sup>	76.83	$(p^{-4})_{10}^+(n^3)_{23/2}^-$	0.0	4.0	1.0	0.0	0.0	1.0	1.0
43/2 <sup>-</sup>	85.12	$(p^{-4})_{12}^+(n^3)_{23/2}^-$	0.0	4.0	1.0	0.0	0.0	1.0	1.0
45/2 <sup>-</sup>	99.91	$(p^{-4})_{12}^+(n^3)_{21/2}^-$	0.0	4.0	1.0	0.0	0.0	1.0	1.0
47/2 <sup>-</sup>	100.0	$(p^{-4})_{12}^+(n^3)_{23/2}^-$	0.0	4.0	0.9	0.0	0.0	1.1	1.0

### E. Level structures of negative-parity states for particle-hole nuclei around $^{100}\text{Sn}$

It can be seen from Fig. 8 that the present  $T = 1$  dominated  $p$ - $n$  quadrupole interaction can reproduce the negative-parity states of particle-hole nuclei around  $^{100}\text{Sn}$  very well [7,9,10]. It is surprising that the calculated levels up to the fully aligned seven-particle  $47/2^-$  state in  $^{99}\text{Pd}$  are in reasonable agreement with the experimental ones. It should be pointed out that the negative-parity sequences do not completely arise from the  $\nu h_{11/2}$ . As indicated in Fig. 8, the  $\pi(p_{1/2}^{-1}g_{9/2}^{-1})_{5^-}$  state in  $^{98}\text{Pd}$  is comparable in energy with the single-neutron state  $11/2^-$  in  $^{99}\text{Pd}$  and  $(\pi g_{9/2}^{-1}\nu h_{11/2})_{8^-}$  in  $^{100}\text{Ag}$ . Therefore, the level structures of negative-parity states for particle-hole nuclei around  $^{100}\text{Sn}$  should involve both the  $\nu h_{11/2}$  and  $\pi p_{1/2}^{-1}$ . Indeed, such excitations can be seen in Table IV. However, the  $p$ - $n$  quadrupole interaction does not induce the proper configuration mixing between the proton and neutron negative-parity components, for example  $(\pi g_{9/2}^{-1}\nu h_{11/2})_{2^-}$  and  $(\pi p_{1/2}^{-1}\nu d_{5/2})_{2^-}$ .

### V. SUMMARY

This paper presents the level-structure study of particle-hole nuclei around  $^{100}\text{Sn}$ . Near yrast positive-parity states are mainly formed by the coupling of  $g_{9/2}$  valence-proton holes to the  $d_{5/2}$  and  $g_{7/2}$  valence-neutron particles. The obvious feature of level structure in this region is the

much higher excitation energy for the fully aligned state involving  $\nu g_{7/2}$  rather than  $\nu d_{5/2}$ . This is attributed to the strong (weak) repulsion between the aligned  $g_{9/2}$  proton hole and  $g_{7/2}$  ( $\nu d_{5/2}$ ) neutron particle. By comparing the pure  $T = 0$  and  $T = 1$   $\pi g_{9/2}^{-1}\nu d_{5/2}$  and  $\pi g_{9/2}^{-1}\nu g_{7/2}$  quadrupole interactions with the experimental multiplets, we estimate that the  $T = 1$  channel should be dominated for the  $p$ - $n$  residual interaction, where the quadrupole-quadrupole term is a main component after extracting the monopole term. The near yrast states are compared with the results of shell model calculations in the model spaces of  $\pi(p_{1/2}, g_{9/2})^{-1--4}$  and  $\nu(d_{5/2}, s_{1/2}, d_{3/2}, g_{7/2}, h_{11/2})^{1-3}$  by using the  $T = 1$  dominant  $p$ - $n$  quadrupole interaction, and the reasonable agreement with each other gives indirect proof of  $T = 1$  dominant level structures of particle-hole nuclei around  $^{100}\text{Sn}$ . The level structures of negative-parity states for particle-hole nuclei around  $^{100}\text{Sn}$  should involve the competition between the  $\nu h_{11/2}$  and  $\pi p_{1/2}^{-1}$  excitations.

### ACKNOWLEDGMENTS

Thanks are given to Prof. M. Hasegawa for providing the interaction code. This work was supported by the National Natural Science Foundation of China (Grant Nos. 10825522, 11175217, GJ073005, 10975163, and 11021504), the Chinese Academy of Sciences, and the Major State Basic Research Developing Program of China (Nos. 2007CB815005 and 2007CB815001).

[1] M. Lipoglavsek, C. Baktash, J. Blomqvist, M. P. Carpenter, D. J. Dean, T. Engeland, C. Fahlander, M. Hjorth-Jensen, R. V. F. Janssens, A. Likar, J. Nyberg, E. Osnes, S. D. Paul,

A. Piechaczek, D. C. Radford, D. Rudolph, D. Seweryniak, D. G. Sarantites, M. Vencelj, and C.-H. Yu, *Phys. Rev. C* **66**, 011302(R) (2002).

- [2] M. Lipoglavsek, C. Baktash, M. P. Carpenter, D. J. Dean, T. Engeland, C. Fahlander, M. Hjorth-Jensen, R. V. F. Janssens, A. Likar, J. Nyberg, E. Osnes, S. D. Paul, A. Piechaczek, D. C. Radford, D. Rudolph, D. Seweryniak, D. G. Sarantites, M. Vencelj, and C.-H. Yu, *Phys. Rev. C* **65**, 021302(R) (2002).
- [3] R. M. Clark, J. N. Wilson, D. Appelbe, M. P. Carpenter, C. J. Chiara, M. Cromaz, M. A. Deleplanque, M. Devlin, R. M. Diamond, P. Fallon, D. B. Fossan, R. V. F. Janssens, D. G. Jenkins, N. Kelsall, T. Koike, D. R. LaFosse, G. J. Lane, I. Y. Lee, A. O. Macchiavelli, D. G. Sarantites, D. Seweryniak, K. Starosta, F. S. Stephens, C. E. Svensson, K. Vetter, R. Wadsworth, J. C. Waddington, D. Ward, I. Wiedenhover, and B. Alex Brown, *Phys. Rev. C* **61**, 044311 (2000).
- [4] M. Palacz, J. Cederkall, M. Lipoglavsek, J. Persson, A. Atac, J. Blomqvist, H. Grawe, C. Fahlander, A. Johnson, A. Kerek, J. Kownacki, A. Likar, L.-O. Norlin, J. Nyberg, R. Schubart, D. Seweryniak, Z. Sujkowski, R. Wyss, G. de Angelis, P. Bednarczyk, Zs. Dombradi, D. Foltescu, D. Jerrestam, S. Juutinen, E. Makela, G. Perez, M. de Poli, H. A. Roth, T. Shizuma, O. Skeppstedt, G. Sletten, S. Tormanen, and T. Vass, *Nucl. Phys. A* **608**, 227 (1996).
- [5] J. Cederkall, M. Lipoglavsek, M. Palacz, J. Persson, J. Blomqvist, A. Atac, C. Fahlander, H. Grawe, A. Johnson, W. Klamra, J. Kownacki, A. Likar, L.-O. Norlin, J. Nyberg, R. Schubart, D. Seweryniak, G. de Angelis, P. Bednarczyk, Zs. Dombradi, D. Foltescu, M. Gorska, D. Jerrestam, S. Juutinen, E. Makela, B. M. Nyako, G. Perez, M. de Poli, H. A. Roth, T. Shizuma, O. Skeppstedt, G. Sletten, and S. Tormanen, *Eur. Phys. J. A* **1**, 7 (1998).
- [6] D. Sohler, Zs. Dombradi, J. Blomqvist, J. Cederkall, J. Huijnen, M. Lipoglavsek, M. Palacz, A. Atac, C. Fahlander, H. Grawe, A. Johnson, A. Kerek, W. Klamra, J. Kownacki, A. Likar, L.-O. Norlin, J. Nyberg, J. Persson, D. Seweryniak, G. de Angelis, P. Bednarczyk, D. Foltescu, D. Jerrestam, S. Juutinen, E. Makela, M. de Poli, H. A. Roth, T. Shizuma, O. Skeppstedt, G. Sletten, J. Timar, S. Tormanen, and M. Weiszflog, *Eur. Phys. J. A* **16**, 171 (2003).
- [7] R. Alfier, D. Alber, H. Grawe, H. Kluge, K. H. Maier, R. Schubart, D. B. Fossan, and W. F. Piel Jr., *Z. Phys. A* **355**, 135 (1996).
- [8] W. F. Piel Jr., D. B. Fossan, R. Ma, E. S. Paul, N. Xu, and J. B. McGrory, *Phys. Rev. C* **41**, 1223 (1990).
- [9] J. Cederkall, G. Perez, M. Lipoglavsek, M. Palacz, J. Persson, A. Atac, J. Blomqvist, C. Fahlander, H. Grawe, A. Johnson, W. Klamra, J. Kownacki, A. Likar, L.-O. Norlin, J. Nyberg, R. Schubart, D. Seweryniak, G. de Angelis, P. Bednarczyk, Zs. Dombradi, D. Foltescu, D. Jerrestam, S. Juutinen, E. Makela, B. M. Nyako, M. de Poli, H. A. Roth, T. Shizuma, O. Skeppstedt, G. Sletten, and S. Tormanen, *Z. Phys. A* **359**, 227 (1997).
- [10] S. Sihotra, Z. Naik, S. Kumar, K. Singh, J. Goswamy, N. Singh, R. Kumar, R. P. Singh, S. Muralithar, R. K. Bhowmik, R. Palit, and D. Mehta, *Phys. Rev. C* **83**, 024313 (2011).
- [11] L. Coraggio, A. Covello, A. Gargano, and N. Itaco, *Phys. Rev. C* **70**, 034310 (2004).
- [12] <http://www.nndc.bnl.gov/ensdf/>.
- [13] Y. H. Zhang, M. Hasegawa, W. T. Guo, M. L. Liu, X. H. Zhou, G. de Angelis, T. M. Axiotis, A. Gadea, N. Marginean, Martinez, D. R. Napoli, C. Rusu, Zs. Podolyak, C. Ur, D. Bazzacco, F. Brandolini, S. Lunardi, S. M. Lenzi, R. Menegazzo, R. Schwengner, A. Gargano, W. von Oertzen, and S. Tazaki, *Phys. Rev. C* **79**, 044316 (2009).
- [14] W. Rae, the paper and the NUSHELLX code in the website <http://knollhouse.org>, released in 2008.
- [15] D. Seweryniak, M. P. Carpenter, S. Gros, A. A. Hecht, N. Hoteling, R. V. F. Janssens, T. L. Khoo, T. Lauritsen, C. J. Lister, G. Lotay, D. Peterson, A. P. Robinson, W. B. Walters, X. Wang, P. J. Woods, and S. Zhu, *Phys. Rev. Lett.* **99**, 022504 (2007).
- [16] D. H. Gloeckner and F. J. D. Serduke, *Nucl. Phys. A* **220**, 477 (1974).
- [17] M. Hasegawa and K. Kaneko, *Phys. Rev. C* **59**, 1449 (1999).
- [18] M. Hasegawa, K. Kaneko, and S. Tazaki, *Nucl. Phys. A* **674**, 411 (2000); **688**, 765 (2001); *Prog. Theor. Phys.* **107**, 731 (2002).
- [19] C. Fahlander, M. Palacz, D. Rudolph, D. Sohler, J. Blomqvist, J. Kownacki, K. Lagergren, L. O. Norlin, J. Nyberg, A. Algora, C. Andreoiu, G. de Angelis, A. Atac, D. Bazzacco, L. Berglund, T. Back, J. Cederkall, B. Cederwall, Zs. Dombradi, B. Fant, E. Farnea, A. Gadea, M. Gorska, H. Grawe, N. Hashimoto-Saitoh, A. Johnson, A. Kerek, W. Klamra, S. M. Lenzi, A. Likar, M. Lipoglavsek, M. Moszynski, D. R. Napoli, C. Rossi-Alvarez, H. A. Roth, T. Saitoh, D. Seweryniak, O. Skeppstedt, M. Weiszflog, and M. Wolinska, *Phys. Rev. C* **63**, 021307(R) (2001).
- [20] M. Gorska, H. Grawe, D. Kast, G. de Angelis, P. G. Bizzeti, B. A. Brown, A. Dewald, C. Fahlander, A. Gadea, A. Jungclaus, K. P. Lieb, K. H. Maier, D. R. Napoli, Q. Pan, R. Peusquens, M. De Poli, M. Rejmund, and H. Tiesler, *Phys. Rev. C* **58**, 108 (1998).
- [21] M. Lipoglavsek, D. Seweryniak, C. N. Davids, C. Fahlander, M. Gorska, R. V. F. Janssens, J. Nyberg, J. Uusitalo, W. B. Walters, I. Ahmad, J. Blomqvist, M. P. Carpenter, J. A. Cizewski, S. M. Fischer, H. Grawe, G. Hackman, M. Huhta, C. J. Lister, D. Nisius, G. Poli, P. Reiter, J. Ressler, J. Schwartz, and A. Sonzogni, *Phys. Lett.* **440B**, 246 (1998).
- [22] K. Sieja, F. Nowacki, K. Langanke, and G. Martinez-Pinedo, *Phys. Rev. C* **79**, 064310 (2009).
- [23] C. Plettner, L. Batist, J. Doring, A. Blazhev, H. Grawe, V. Belleguic, C. R. Bingham, R. Borcea, M. Gierlik, M. Gorska, N. Harrington, Z. Janas, M. Karny, R. Kirchner, C. Mazzocchi, P. Munro, E. Roeckl, K. Schmidt, and R. Schwengner, *Phys. Rev. C* **66**, 044319 (2002).